Supplementary Online Content

Schreiber S, Schreiber F, Lockhart SN, et al; Alzheimer's Disease Neuroimaging Initiative. Alzheimer disease signature neurodegeneration and *APOE* genotype in mild cognitive impairment with suspected non–Alzheimer disease pathophysiology. *JAMA Neurol.* Published online March 20, 2017. doi:10.1001/jamaneurol.2016.5349

This supplementary material has been provided by the authors to give readers additional information about their work.

eAppendix. Supplemental Material and Methods

Subjects and Methods

Data used in the preparation of this article were obtained from the Alzheimer's Disease Neuroimaging Initiative (ADNI) database (adni.loni.usc.edu). The ADNI was launched in 2003 as a public-private partnership, led by Principal Investigator Michael W. Weiner, MD. The primary goal of ADNI has been to test whether serial magnetic resonance imaging (MRI), positron emission tomography (PET), other biological markers, and clinical and neuropsychological assessment can be combined to measure the progression of mild cognitive impairment (MCI) and early Alzheimer's disease (AD).

To be precise, ADNI is a multisite study using the modalities of Aβ imaging (with [^{18}F] florbetapir), glucose metabolism (using [^{18}F] FDG), MRI, CSF, and cognitive measurements. ADNI is supported by the National Institutes of Health, private pharmaceutical companies, and nonprofit organizations with approximately 50 medical center and university sites across the United States and Canada (http://adni.loni.usc.edu). Full inclusion/exclusion criteria are available at www.adni-info.org. To summarize, all participants were aged between 55 and 90 years, had completed at least 6 years of education, were fluent in English or Spanish, and had no further relevant neurological diseases.

APOE results were obtained using DNA from blood samples. Eleven MCI subjects (Aβ+N- n=4, Aβ-N+ n=1, Aβ+N+ n=6) but none of the cognitively normal subjects (CN) had APOE ε2/4 genotypes; these were coded as positive for each allele. In MCI and CN there were no homozygous APOE ε2 carriers; while there were n=47 MCI homozygous APOE ε4 carriers (Aβ-N- n=3, Aβ+N- n=10, Aβ-N+ n=3, Aβ+N+ n=31) and n=6 CN homozygous APOE ε4 carriers (Aβ-N- n=1, Aβ+N- n=1, Aβ-N+ n=1, Aβ+N+ n=3).

Cognitively normal subjects and MCI cases underwent their baseline [^{18}F] florbetapir scan between 05/2010 and 11/2013. Cognitively normal subjects were free of memory complaints, had a Mini-Mental State Exam (MMSE) score between 24 and 30 and a Clinical Dementia Rating (CDR) of 0; MCI subjects were classified as single- or multidomain amnestic, had a subjective memory complaint, a MMSE score between 24 and 30, and a CDR of 0.5. EMCI and LMCI patients differed only in their education-adjusted scores on the Logical Memory II

subscale (Delayed Paragraph Recall, Paragraph A only) from the Wechsler Memory Scale – Revised [1].

[^{18}F] Florbetapir PET

[^{18}F] florbetapir ADNI data were acquired using different PET scanners at various sites. Images were obtained in four 5-minute frames 50 to 70 minutes after injection of approximately 10 mCi of [^{18}F] florbetapir; the four frames were co-registered to each other, averaged, interpolated to a uniform image and voxel size (160 × 106 × 96, 1.5 mm ^{3}), and smoothed to a uniform resolution (8mm full width at half-maximum [FWHM]) to account for resolution differences between scanners [2]. To quantify cortical amyloid retention, these preprocessed [^{18}F] florbetapir image data and co-registered structural MRI were analyzed as described previously [3,4]. Briefly, using FreeSurfer version 4.5.0 [5] magnetization-prepared rapid gradient echo (MPRAGE) scans from a 3T MRI scan within 2 months of [^{18}F] florbetapir scans were segmented and parcellated into individual cortical regions, used to extract the mean [^{18}F] florbetapir uptake from the gray matter of lateral and medial frontal, anterior, and posterior cingulate, lateral parietal, and lateral temporal regions.

[^{18}F] FDG PET

FDG image data (closest to baseline [^{18}F] florbetapir scan) were obtained at ADNI sites and were acquired 30 to 60 minutes postinjection, downloaded from the ADNI website after preprocessing (frame averaging, spatial alignment, interpolation to a standard voxel size, smoothing to a common resolution of 8mm FWHM), and then spatially normalized to a standard ^{15}O-H_2O PET template in MNI coordinate space using SPM5 (Wellcome Trust Centre for Neuroimaging, Institute of Neurology at University College London) [6].

Structural MRI

Non-accelerated sagittal volumetric 3-dimensional (3D) MPRAGE 3T images were acquired at each site and scans closest to baseline [^{18}F] florbetapir PET images were taken for analysis. Baseline white matter hyperintensity (WMH) volume measurement approach included the linear co-registration of the preprocessed fluid attenuation inversion recovery (FLAIR) and the preprocessed 3D MPRAGE images, the alignment of each 3D MPRAGE scan to a minimum

deformation template (MDT), the estimation (segmentation) of FLAIR WMH in standard space using a modified Bayesian probability structure based on prior WMH probability maps to create a binary WMH mask, and the back-transformation of the segmented WMH mask into native space for tissue volume calculation, as described previously [7]. WMH volume was adjusted by ICV derived from an automatic four tissue segmentation (white matter, gray matter, CSF, WMH) using Bayesian maximum likelihood expectation maximization (EM) computation, implemented at the Imaging of Dementia and Aging (IDeA) laboratory at the University of California, Davis.

Cerebrospinal fluid

CSF parameters were measured using the multiplex xMAP Luminex platform (Luminex Corp, Austin, TX) with Innogenetics (INNO-BIA AlzBio3; Ghent, Belgium; for research use–only reagents) immunoassay kit–based reagent 34-36. Analysis details and quality control procedures are available at http://adni.loni.ucla.edu. All CSF aliquots were anchored to the same baseline assay values derived from the original ADNI1 dataset to use the cutoff values for abnormal and normal $A\beta_{1-42}$, t-tau and p-tau_{181p}, established and validated for that assay [8].

Image Biomarker Cutoffs

The threshold for a positive [^{18}F] florbetapir SUVR was 1.11 [4], which is based on the upper limit of the 95% CI for the [^{18}F] florbetapir distribution values in young healthy controls [9], and which is also consistent with a separate autopsy-validated sample [10].

Statistics

For mixed effects linear models, group was included as a set of pairwise dummy variables with Aβ- subjects as reference (coded as 0), and Aβ+ cases taken as group of interest (coded as 1), relating Aβ-N+ to Aβ+N+ or Aβ-FDG+ to Aβ+FDG+ or Aβ-HV+ to Aβ+HV+ participants. The same approach was conducted comparing Aβ-N+APOEε2- (coded as 0) against Aβ-N+APOEε2+ (coded as 1) and Aβ-N+APOEε4- (coded as 0) against Aβ-N+APOEε4+ (coded as 1) cases. Estimates demonstrate the differences between the mean score of the group of interest and our respective reference subjects.

eTable 1. Cluster Peak Voxels in MCI Aβ-N+ Individuals and in MCI Aβ-N+APOE ε4 Noncarriers

Contrast	Cluster number	Cluster size (k)	t-value	MNI coordinates			Labeling	Other regions included in the Cluster (larger 10% Cluster)
				x	y	z		
FDG voxelwise							**Aβ-N+ > Aβ+N+**	
Aβ-N+ > Aβ+N+	1	(7352)	5.6	-6	-70	36	L precuneus	R superior temporal gyrus, R precuneus, R angular gyrus
	2	(307)	5.0	-58	-46	-20	L inferior temporal gyrus	
Aβ-FDG+ > Aβ+FDG+	1	(2428)	5.2	-6	-70	36	L precuneus	R precuneus, R superior temporal gyrus
	2	(1171)	5	-42	-74	42	L angular gyrus	L middle temporal gyrus, L supramarginal gyrus, L superior parietal gyrus
Aβ-HV+ > Aβ+HV+	1	(1219)	4.9	-44	-50	22	L angular gyrus	L middle temporal gyrus, L supramarginal gyrus
	2	(288)	4.5	-60	-48	-18	L inferior temporal gyrus	
	3	(2180)	4.3	20	-60	50	R superior parietal gyrus	L precuneus, R superior temporal gyrus, R precuneus, R inferior parietal gyrus
VBM							**Aβ-N+ > Aβ+N+**	
Aβ-N+ > Aβ+N+	1	(3209)	5.0	-57	-40	8	L middle temporal gyrus	
Aβ-FDG+ > Aβ+FDG+	1	(2310)	5.3	-51	-48	2	L middle temporal gyrus	
Aβ-HV+ >	1	(3131)	5.2	-	-	9	L middle	

Aβ+HV+				56	42		temporal gyrus	
FDG voxelwise							**Aβ-N+APOEε4- > Aβ-**	
N+APOEε4+								
Aβ-N+APOEε4- > Aβ-N+APOEε4+	1	(353)	4.7	0	-58	36	L precuneus	R precuneus

Aβ, β-amyloid; APOE, apolipoprotein E; FDG, [^{18}F]-Fluorodeoxyglucose; HV, hippocampal volume; L, left; N, neurodegeneration; R, right; VBM, voxel-based morphometry; significant at p 0.001 uncorrected voxel-level, p 0.05 FWE corrected cluster-level, k 260

eTable 2. Baseline Variables in Cognitively Normal Aβ-N+ Subtypes Compared With Their Aβ Positive Counterparts

	Aβ-N+ n = 52	**Aβ+N+ n = 37**	***P* Value**	**Aβ-FDG+ n = 30**	**Aβ+FDG+ n = 22**	**p**	**Aβ-HV+ n = 33**	**Aβ+HV+ n = 26**	***P* Value**
Age at baseline [^{18}F] florbetapir scan, yr	74.5 [7]	77.7 [6.5]	.03	73.9 [7.2]	76.8 [6.4]	0.1	75.5 [6.6]	78.7 [6.3]	.07
Male gender, No. (%)	34 (65)	18 (49)	.1	21 (70)	9 (41)	0.04	22 (67)	15 (58)	.5
Education, yr	16.9 [2.5]	16.5 [3]	.5	16.3 [2.6]	15.9 [3.3]	0.6	17.1 [2.2]	16.7 [3.2]	.6
APOEε2 carriers, No. (%)	7 (14)	2 (5)	.3	6 (20)	1 (5)	0.2	3 (9)	2 (8)	1.0
APOEε4 carriers, No. (%)	11 (21)	20 (54)	<.001	7 (23)	11 (50)	0.02	7 (21)	13 (50)	.007
Mean FDG (meta-ROIs)	1.26 [0.1]	1.24 [0.1]	.5	1.19 [0.05]	1.17 [0.06]	0.3	1.3 [0.1]	1.27 [0.1]	.4
HV/ICV (ROI)	4.7×10^{-3} [0.7×10^{-3}]	4.5×10^{-3} [0.5×10^{-3}]	.7	5×10^{-3} [0.7×10^{-3}]	4.7×10^{-3} [0.5×10^{-3}]	0.2	4.2×10^{-3} [0.3×10^{-3}]	4.3×10^{-3} [0.3×10^{-3}]	.2
CSF t-tau, pg/ml	57.6 [24.9]	83.9 [40]	.03	54.7 [24.4]	81.2 [31.5]	0.008	63 [23.2]	82.8 [45]	.3
CSF p-tau$_{181p}$, pg/ml	29.6 [10.7]	41.4 [21.6]	.03	27.9 [10.7]	37.6 [17.1]	0.06	33.8 [10]	39.7 [23.4]	.5
WMH% of ICV	3.4×10^{-3} [4.5×10^{-3}]	8.8×10^{-3} [13.7×10^{-3}]	.008	3.1×10^{-3} [2.7×10^{-3}]	9.1×10^{-3} [16×10^{-3}]	0.06	3.5×10^{-3} [5.2×10^{-3}]	10.8×10^{-3} [16×10^{-3}]	.01
aHTN, No. (%)	22 (42)	19 (51)	.4	12 (40)	12 (55)	0.4	12 (36)	12 (46)	.3
Family history of AD, No. (%)	18 (35)	18 (49)	.06	10 (33)	14 (64)	0.03	12 (36)	11 (42)	.3
Progression to MCI/AD, No. (%)	7 (13)	11 (30)	.1	3 (10)	6 (27)	0.08	6 (18)	9 (35)	.5
ADAS-cog (baseline)	5.2 [2.9]	6.9 [3]	.007	5.4 [3.2]	7.1 [3.4]	0.05	5.3 [2.9]	7.3 [3]	.01
AVLT (baseline)	47.5 [12.1]	44.4 [9.4]	.3	48.3	43.3 [9.9]	0.2	46.1	43.7 [9.8]	.5

				[13.1]			[11.6]	
Group x time on ADAS-cog	e -0.3 [0.3]		.2	e -0.4 [0.6]		0.5	e -0.5 [0.4]	.1
Group x time on AVLT	e -1.3 [0.9]		.1	e -1.6 [1.2]		0.2	e -0.7 [0.9]	.4

Aβ, β-amyloid; AD, Alzheimer's disease; ADAS-cog, Alzheimer's disease assessment scale cognitive subscale; aHTN, arterial hypertension; APOE, apolipoprotein E; AVLT, Auditory Verbal Learning Test; CSF, cerebrospinal fluid; FDG, ^{18}F-Fluorodeoxyglucose; HV, hippocampal volume; ICV, intracranial volume; MCI, mild cognitive impairment; meta-ROIs, meta-regions of interest; N, neurodegeneration; p-tau$_{181p}$, tau phosphorylated at threonine 181; t-tau, total tau; WMH, white matter hyperintensities; Bonferroni-adjusted *P* values are significant at ⩽.003 (for cross-sectional analysis) or at ⩽.008 (for longitudinal analysis) (see Material & Methods).

eFigure 1. Patterns of Neurodegeneration in Individuals With β-Amyloid Peptide–Positive (Aβ+) and Neurodegeneration-Positive (N+) Subtypes of Mild Cognitive Impairment Compared With Their Aβ- Counterparts

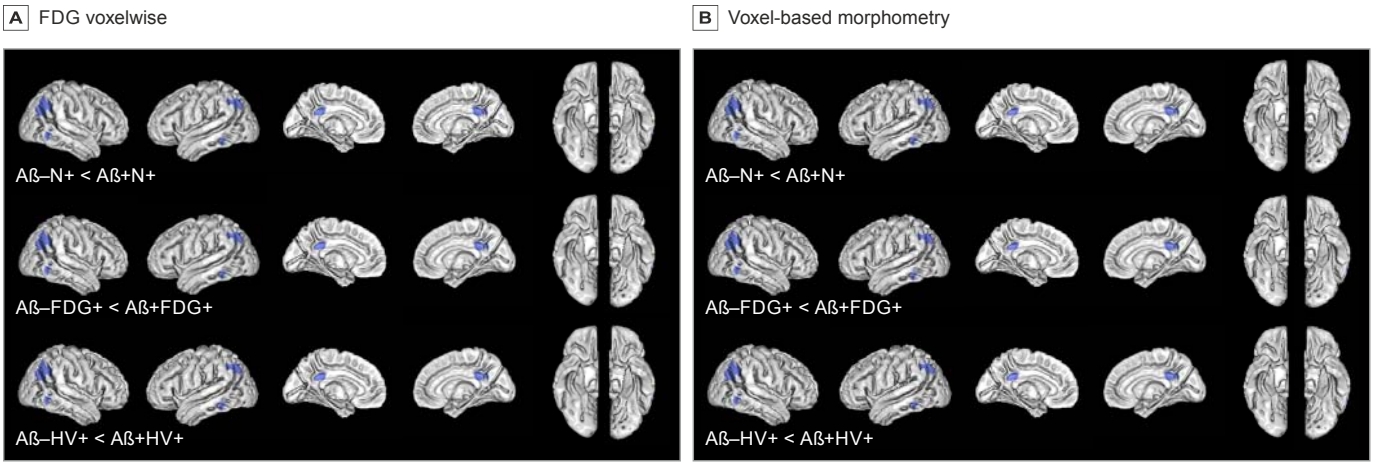

A, Brain surface images demonstrating the results of 3 contrasts in the whole-brain fluorodeoxyglucose F 18–labeled (FDG) voxelwise analysis. B, Brain surface images demonstrating the results of 3 contrasts in voxel-based morphometry. Red indicates clusters that met the significant cluster-level threshold of $P < .05$ corrected (voxelwise threshold $P < .001$ uncorrected, k = 260 voxels). The blue regions of interest (ROIs) represent prespecified meta-ROIs (bilateral inferior temporal gyrus, bilateral angular gyrus, and bilateral posterior-cingulate precuneus region) used to create mean FDG as a composite measure. There were no regions in which Aβ−N+ 16 individuals showed lower FDG metabolism and lower gray matter volume than did Aβ+N+ individuals. HV indicates hippocampal volume.

eFigure 2. Patterns of Glucose Metabolism in β-Amyloid Peptide–Negative (Aβ−) and Neurodegeneration-Positive (N+) Carriers of *APOE* ε4 With Mild Cognitive Impairment Noncarriers Compared With Aβ−N+ Noncarriers of *APOE* ε4

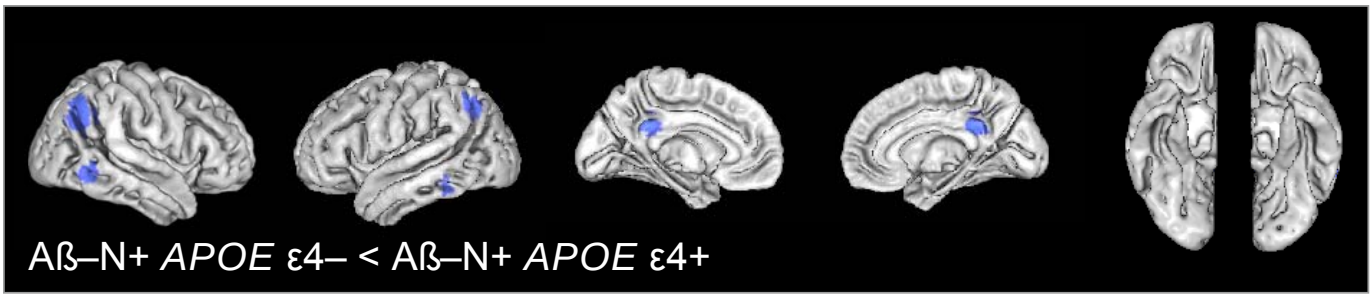

Brain surface images demonstrate the results of whole-brain fluorodeoxyglucose F 18–labeled (FDG) voxelwise analysis in Aβ−N+ carriers of *APOE* ε4 contrasted against Aβ−N+ noncarriers of *APOE* ε4. Red indicates clusters that met the significant cluster-level threshold of $P < .05$ corrected (voxelwise threshold $P < .001$ uncorrected, k = 260 voxels). The blue regions of interest (ROIs) represent prespecified meta-ROIs. There were no regions in which *APOE* ε4− individuals showed lower glucose metabolism than did *APOE* ε4+ individuals.

eFigure 3. *APOE*-Dependent Alzheimer Disease (AD) Signature Patterns of Neurodegeneration in Individuals With β-Amyloid Peptide–Negative (Aβ−) and Neurodegeneration-Positive (N+) Mild Cognitive Impairment (MCI)

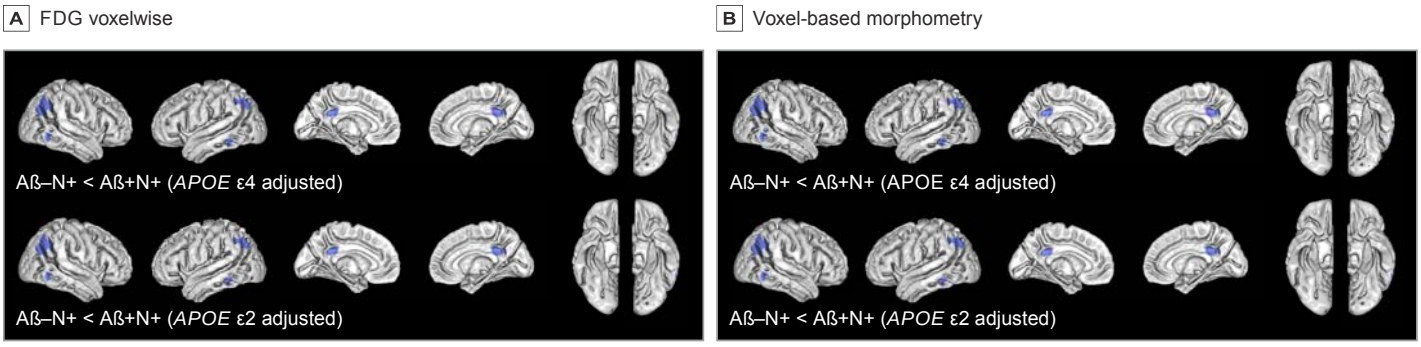

A, Brain surface images demonstrating the results of whole-brain fluorodeoxyglucose F 18–labeled (FDG) voxelwise analysis (cluster-level threshold $P < .05$ corrected; voxelwise threshold $P < .001$ uncorrected, k = 260 voxels). B, Brain surface images demonstrating the results of voxel-based morphometry (cluster-level threshold $P < .05$ corrected; voxelwise threshold $P < .001$ uncorrected, k = 260 voxels). The blue regions of interest (ROIs) represent prespecified meta-ROIs. There were no regions in which Aβ−N+ individuals showed lower FDG metabolism and lower gray matter volumes than did Aβ+N+ individuals after inclusion of *APOE* ε4 or *APOE* ε2 carrier status as additional variables.

eReferences

1. Wechsler D. Wechsler Adult Intelligence Scale-3rd Edition. San Antonio, TX: Harcourt Assessment., 1997.
2. Joshi A, Koeppe RA, Fessler JA. Reducing between scanner differences in multi-center PET studies. Neuroimage 2009; 46(1):154-159.
3. Landau SM, Mintun MA, Joshi AD, Koeppe RA, Petersen RC, Aisen PS et al. Amyloid deposition, hypometabolism, and longitudinal cognitive decline. Ann Neurol 2012; 72(4):578-586.
4. Landau SM, Lu M, Joshi AD, Pontecorvo M, Mintun MA, Trojanowski JQ et al. Comparing positron emission tomography imaging and cerebrospinal fluid measurements of beta-amyloid. Ann Neurol 2013; 74(6):826-836.
5. Fischl B, Salat DH, Busa E, Albert M, Dieterich M, Haselgrove C et al. Whole brain segmentation: automated labeling of neuroanatomical structures in the human brain. Neuron 2002; 33(3):341-355.
6. Ashburner J, Friston KJ. Unified segmentation. Neuroimage 2005; 26(3):839-851.
7. Schwarz C, Fletcher E, DeCarli C, Carmichael O. Fully-automated white matter hyperintensity detection with anatomical prior knowledge and without FLAIR. Inf Process Med Imaging 2009; 21:239-251.
8. Shaw LM, Vanderstichele H, Knapik-Czajka M, Clark CM, Aisen PS, Petersen RC et al. Cerebrospinal fluid biomarker signature in Alzheimer's disease neuroimaging initiative subjects. Ann Neurol 2009; 65(4):403-413.
9. Joshi AD, Pontecorvo MJ, Clark CM, Carpenter AP, Jennings DL, Sadowsky CH et al. Performance characteristics of amyloid PET with florbetapir F 18 in patients with alzheimer's disease and cognitively normal subjects. J Nucl Med 2012; 53(3):378-384.
10. Clark CM, Schneider JA, Bedell BJ, Beach TG, Bilker WB, Mintun MA et al. Use of florbetapir-PET for imaging beta-amyloid pathology. JAMA 2011; 305(3):275-283.